Non-invasive Extraction of Physiological Parameters in Quantitative PET Studies Using Simultaneous Estimation and Cluster Analysis

Koon-Pong Wong[1,2], Dagan Feng[1,3], Steven R. Meikle[2], and Michael J. Fulham[2,4]
[1]Basser Department of Computer Science, The University of Sydney, NSW 2006, Australia
[2]Department of PET and Nuclear Medicine, Royal Prince Alfred Hospital, Camperdown, NSW 2050, Australia
[3]Department of Electronic and Information Engineering, The Hong Kong Polytechnic University, Hong Kong
[4]Faculty of Medicine, The University of Sydney, NSW 2006, Australia

Abstract

Quantitative PET studies usually require invasive blood sampling from a peripheral artery to obtain an input function for accurate modelling. However, blood sampling is impractical in clinical PET studies. We recently proposed a non-invasive modelling approach that can simultaneously estimate parameters which describe both the input and output functions using two or more regions of interest (ROIs). However, this approach is still limited by manual delineation of ROIs which is subjective and time-consuming. In this work, we present an extension to our method where ROI delineation is performed automatically by cluster analysis so that subjectivity is reduced while at the same time ensuring that the extracted time-activity curves have distinct kinetics. Our aim was to investigate the feasibility of using the kinetics extracted by cluster analysis for non-invasive quantification of physiological parameters. The estimates and the fitted curves obtained by simultaneous estimation are in good agreement with those obtained by model fitting with the measured input function (*gold standard* method). We conclude that cluster analysis is able to identify distinct kinetics and hence can be used for the non-invasive quantification of physiological parameters.

I. Introduction

Positron emission tomography (PET) with [^{18}F]-fluorodeoxyglucose (FDG) has been widely used for the study of neurologic disorders, cardiac disease and cancer because it provides pathophysiological information that is not available from anatomical imaging modalities such as magnetic resonance (MR) and computed tomography (CT). Various approaches including qualitative, semi-quantitative and quantitative methods, have been proposed for the analysis of PET data. It is believed that quantitative PET can provide more accurate and detailed diagnostic information about the uptake characteristics of a variety of tracers despite the complicated experimental procedures. The assessment of treatment response in neurological and oncological conditions offers an important potential application of quantitative PET. However, one of the major disadvantages is the requirement for measurement of the input function (IF) for accurate modelling. The *gold standard* method is to obtain the IF by frequent blood sampling from a peripheral artery under local anaesthesia [1]. However, arterial catheterisation is invasive and frequent blood sampling may result in increased radiation exposure to PET personnel. Therefore, full arterial blood sampling is usually not performed in routine clinical PET studies.

A number of approaches have been proposed to reduce the need for arterial blood sampling [2–8]. We recently proposed a simultaneous estimation (SIME) approach to estimate the IF and the kinetic model parameters from two or more ROIs, making use of one or more late venous blood samples for calibration [9]. We modified the method to improve the reliability of parameter estimation (SIMEP) and our results with *in-vivo* PET data are promising [10]. The method is still limited, however, by the selection of ROIs whose time-activity curves (TACs) must have distinct kinetics so that the physiological parameters in the impulse response functions (IRFs) obtained by SIME are numerically identifiable. The ROIs are usually drawn manually on the PET images but this process requires skilled operators, reproducibility is difficult to measure and it is time-consuming. This study presents a further extension whereby tissue TACs are extracted automatically from dynamic PET data by cluster analysis which is used to segment tissues with different kinetics. Our aim is to investigate the feasibility of using the kinetics extracted by cluster analysis for non-invasive quantification of physiological parameters.

II. Materials and Methods

A. Simultaneous Estimation of Physiological Parameters and Input Function

We have reported the Monte-Carlo simulations [9] and the *in-vivo* FDG-PET studies that validate our method [10]. Only a brief summary of the method is presented here. We first assume that (1) all the tissue TACs are driven by the same IF, (2) the information of the IF is embedded in the tissue TACs, and (3) the parameters in the IF and the IRFs are identifiable. The main aim is to make use of the multiple tissue TACs that can be obtained by defining different ROIs on the dynamic PET images to recover the IF embedded in the tissue TACs. Since the TACs are the convolution integration of the IF with the IRFs of the corresponding ROIs, it is possible to estimate the IRF parameters and the IF by minimising the errors between the

0-7803-6503-8/01/$10.00 2001 IEE

model predicted tissue response and the corresponding measurements in two or more ROIs simultaneously.

In order to improve the numerical identifiability of the parameters to be estimated, one or two late venous blood samples are required to calibrate the estimated IF [9,10]. Nonlinear least squares (NLLS) is used to optimise the IF and the IRF parameters based on the following cost function:

$$\Phi(\boldsymbol{\theta}) = \sum_{i=1}^{N}\sum_{j=1}^{M}\left[\left(\hat{c}_p^*(t)\otimes h_i(t)\right)\otimes\delta(t-t_j') - c_{T_i}^*(t_j')\right]^2 + \sum_{k=1}^{m} w_k\left[\hat{c}_p^*(t_k) - \bar{c}_p^*(t_k)\right]^2 \quad (1)$$

where N is the total number of ROIs incorporated into the model fitting procedure; M is the number of frames for each tissue TAC; $h_i(t)$ is the IRF of the i-th ROI; $\boldsymbol{\theta}$ denotes the vector of parameters to be estimated; $\delta(t-t_j')$ is a Dirac delta function shifted in time by t_j' units; $\otimes$ is the convolution integral operator; $\hat{c}_p^*(t)$ is the estimated arterial IF; m is the number of venous blood samples taken late in the course of the study for calibration; $\bar{c}_p^*(t_k)$ is the tracer concentration in plasma measured at time t_k ($k = 1, 2, \ldots, m$); and w_k is chosen to be 100 so that the late venous samples, $\bar{c}_p^*(t_k)$, are given more weight as they are usually more reliable than the PET measurements. This method is referred to as simultaneous estimation (SIME) [10].

Although precise parameter estimates can be obtained theoretically with SIME, we found that the estimation of the standard deviations for the parameter estimates are usually very poor even though the values of the parameter estimates are accurate [10]. This may be because a large number of noisy data are fitted simultaneously and the information matrix may be poorly-conditioned since the stability of its Jacobian matrix is disrupted by noise. Another possibility could be the high nonlinearity of the parameter space. We have developed a technique that is applied after SIME for the above situations and we refer to this method as post-estimation (SIMEP) [10] in which the parameters in the IRFs are estimated separately by using the estimated IF from SIME and the individual tissue TACs as input-output pairs. The standard deviations of the parameters can be greatly improved due to the reduction in dimensionality of parameter space.

B. *Automatic Extraction of Tissue TACs*

Cluster analysis is used to extract the different kinetics present in dynamic PET data based on the shape and magnitude of the tissue TACs. By assuming that there exists k characteristic kinetics in the PET data, the tissue TACs with similar shape and magnitude can be classified into the same cluster whose kinetics (cluster centroids) are the average of the constituent tissue TACs. Those TACs with different shape and magnitude are classified into different clusters so that the weighted residual sum of squares (WRSS) and the WRSS within a cluster are minimised [11]. Since there may not be *a priori* known about the value of k, it is safer to vary the value of k over a range of integers so that the possible optimum segmentation (thus the optimum value of k) of the data set is covered [11]. The method is similar to the one proposed by Ashburner *et al.* [12] in that there is a finite number of kinetics present in the dynamic PET data. The difference is that the algorithm of Ashburner *et al.* maximises the probability of an arbitrary selected TAC from the data belonging to a specified cluster while the method used in this work minimises the WRSS for an arbitrary selected TAC to its cluster centroid.

Figure 1: A modified template in a slice of the Hoffman brain phantom. A tumour in white matter (white arrow) and an adjacent hypometabolic region (shaded region) in the left middle temporal gyrus are shown.

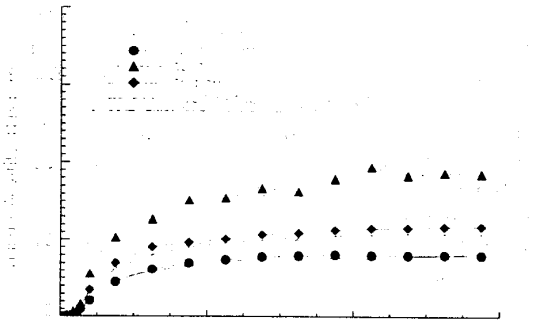

Figure 2: Simulated noisy FDG kinetics in grey matter, white matter, tumour, thalamus, and hypometabolic region adjacent to the tumour.

C. *Simulation*

A slice of the numerical Hoffman brain phantom [13] was modified using a template consisting of five different kinetics (grey matter, white matter, thalamus, tumour in white matter and an adjacent hypometabolic region in left middle temporal gyrus), as shown in Figure 1. The activities in grey matter and white matter were generated using a 5-parameter 3-compartment FDG model [14] with a measured arterial IF obtained from a patient (constant infusion of 400 MBq of FDG over 3

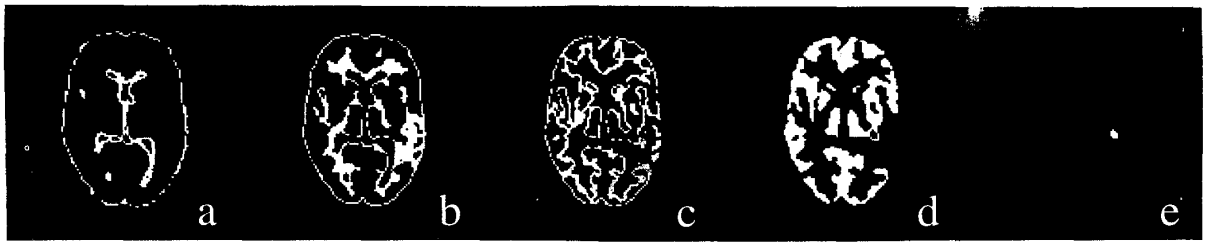

Figure 3: Five cluster images were generated by applying the clustering algorithm to the simulated dynamic FDG-PET data set. The images correspond to: (a) ventricles and scalp, (b) white matter and left middle temporal gyrus, (c) partial volume between grey matter and white matter, (d) grey matter and deep nuclei, and (e) tumour.

minutes), and two 'blood samples' obtained at 30 min and 60 min (i.e. $m = 2$) were used as calibration factors to improve the numerical identifiability. The kinetics present in the hypometabolic region, thalamus and tumour were set to 0.7, 1.1 and 2.0 times the activity in grey matter. The kinetics were then assigned to each brain region and a dynamic sequence of sinograms (22 frames, 6 × 10 sec, 4 × 30 sec, 1 × 120 sec, 11 × 300 sec) was obtained by forward projecting the images into 3.13 mm bins on a 192 × 256 grid. Poisson noise and blurring were also added to simulate realistic sinograms acquired on an ECAT 951R whole body tomograph (CTI/Siemens, Knoxville, TN). Dynamic images were reconstructed using filtered back-projection (FBP) with Hann filter cut-off at the Nyquist frequency. The noisy kinetics are shown in Figure 2 and some of the kinetics are similar to each other due to the added noise and gaussian blurring, although their kinetics are different in the absence of noise. This is illustrated in the white matter and the hypometabolic region, and the grey matter and thalamus.

Since there is no *a priori* knowledge about the optimum number of clusters in practice, the value of k has to be varied so that the unknown value of k which yields the optimum segmentation can be determined [11]. The value of k was varied from 3 to 10, and only those TACs with the most distinct kinetics were selected. This is in contrast to our previous work where TACs with different kinetics were selected from a collection of TACs obtained by manually placing ROIs over the PET images [10]. The selected TACs were then used by SIME and SIMEP for non-invasive estimation of the physiological parameters. Compartmental model fitting to the three TACs with the measured IF (*gold standard* method) was also performed to assess the agreement between the parameter estimates obtained from different methods.

III. Results and Discussion

By applying the cluster algorithm to the noisy dynamic images, five cluster images (corresponding to the best segmentation in this study) were generated (see Figure 3) and their associated TACs were extracted. Three (grey matter, white matter and tumour) out of the five extracted TACs were selected because they possess different kinetics and represent different anatomical regions. The images in Figure 3 are arranged in ascending order (from left to right) according to their total sum of activity. It shows that the clustering algorithm performed well in extracting the underlying tissue kinetics in grey matter, white matter, and tumour. However, the kinetics in the thalamus and the hypometabolic region were not separated from those in grey and white matter. This is not surprising because their kinetics are very similar in the raw PET images (Figure 2). Owing to the partial volume effects, there exists some vague regions whose kinetics are indeterminate (Figure 3(c)) and do not approach grey or white matter. The algorithm is unlikely to assign such kinetics to the cluster corresponding to white matter or to the cluster corresponding to grey matter since the overall segmentation results would be deteriorated. Thus, a cluster is formed to account for the indeterminate kinetics.

Table 1 summarises the estimated physiological parameters, $K = k_1^* k_3^* / (k_2^* + k_3^*)$, in the three TACs using different methods (SIME, SIMEP, and the *gold standard* method). It is seen that the estimates obtained from different methods are in good agreement. The coefficients of variation (CVs) of the K estimates, however, are quite different and varied with different methods. The worst CVs were those obtained with SIME, while the intermediates were those obtained with SIMEP, and, as expected, the CVs obtained from the *gold standard* method were the best. The results agree with our *in-vivo* data reported previously [10]. Nevertheless, the CVs obtained by SIMEP are reasonable and are much better than those obtained from using SIME despite them being relatively larger than those obtained with the *gold standard* method. This finding is not unexpected because only the tissue kinetics and the two 'blood samples' are available for parameter estimation. In contrast, with the *gold standard* approach the entire measured IF is available in addition to the tissue kinetics. Given the very limited information available, the CVs obtained by SIMEP are acceptable. The three extracted TACs and the corresponding fitted curves by SIME are shown in Figure 4. It is apparent

Table 1
Estimates for the physiological parameter, K, in the three TACs using different methods. Values are estimates ± %CV.

	gold standard	SIME	SIMEP
Grey Matter	0.0109±3.2	0.0102±1001.9	0.0113±8.7
White Matter	0.0075±10.6	0.0076±1223.5	0.0075±29.6
Tumour	0.0219±19.5	0.0203±1228.8	0.0201±15.3

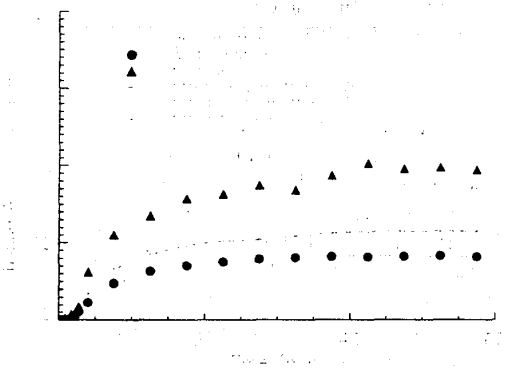

Figure 4: Extracted tissue TACs corresponding to grey matter, white matter and tumour by cluster analysis and the fitted curves obtained by SIME.

that the fitted curves are in good agreement with the corresponding kinetic curves extracted by cluster analysis.

Thus, our results show that the tissue TACs can be extracted automatically by cluster analysis, and the subjectivity of manual ROI delineation is minimised. Cluster analysis can segment tissues of different kinetics in PET data and is a reliable alternative to manual ROI delineation.

IV. Conclusions

Our results show that it is feasible to estimate the physiological parameters with SIME (and SIMEP) using the TACs extracted automatically by cluster analysis. The physiological parameters in different TACs estimated by SIME and SIMEP are comparable to those obtained from model fitting to the TACs with the measured input function (*gold standard*). Although this work used FDG-PET as an example for illustration, it is expected that the methodologies can be applied to PET studies with other tracers.

V. Acknowledgements

This work was supported by the National Health and Medical Research Council (NHMRC) of Australia under Grant No. 980042.

VI. References

[1] M. Reivich, D. E. Kuhl, A. Wolf, J. H. Greenberg, M. E. Phelps, T. Ido, V. Casella, J. Fowler, E. J. Hoffman, A. Alavi, P. Som, and L. Sokoloff, "The [^{18}F] fluorodeoxyglucose method for the measurement of local cerebral glucose utilization in man," *Circ. Res.*, vol. 44, pp. 127–137, 1979.

[2] M. E. Phelps, S. C. Huang, E. J. Hoffman, C. Selin, L. Sokoloff, and D. E. Kuhl, "Tomographic measurement of local cerebral glucose metabolic rate in humans with (F-18)2-fluoro-2-deoxy-D-glucose: Validation of method," *Ann. Neurol.*, vol. 6, pp. 371–388, 1979.

[3] S. C. Huang, M. E. Phelps, E. J. Hoffman, K. Sideris, C. Selin, and D. E. Kuhl, "Noninvasive determination of local cerebral metabolic rate of glucose in man," *Am. J. Physiol.*, vol. 238, pp. E69–E82, 1980.

[4] S. Takikawa, V. Dhawan, P. Spetsieris, W. Robeson, T. Chaly, R. Dahl, D. Margouleff, and D. Eidelberg, "Noninvasive quantitative fluorodeoxyglucose PET studies with an estimated input function derived from a population-based arterial blood curve," *Radiology*, vol. 188, pp. 131–136, 1993.

[5] R. L. Phillips, C. Y. Chen, D. F. Wong, and E. D. London, "An improved method to calculate cerebral metabolic rates of glucose using PET," *J. Nucl. Med.*, vol. 36, no. 9, pp. 1668–1679, 1995.

[6] S. Eberl, A. R. Anayat, R. R. Fulton, P. K. Hooper, and M. J. Fulham, "Evaluation of two population-based input functions for quantitative neurological FDG PET studies," *Eur. J. Nucl. Med.*, vol. 24, no. 3, pp. 299–304, 1997.

[7] K. Chen, D. Bandy, E. Reiman, S. C. Huang, M. Lawson, D. Feng, L. S. Yun, and A. Palant, "Noninvasive quantification of the cerebral metabolic rate for glucose using positron emission tomography, ^{18}F-fluoro-2-deoxyglucose, the Patlak method, and an image-derived input function," *J. Cereb. Blood Flow Metab.*, vol. 18, pp. 716–723, 1998.

[8] M. C. Asselin, V. J. Cunningham, N. Turjanski, L. M. Wahl, P. M. Bloomfield, R. N. Gunn, and C. Nahmias, "Venous sinuses vs. on-line arterial sampling as input functions in PET," *J. Cereb. Blood Flow Metab.*, vol. 19, no. suppl. 1, pp. S791, 1999.

[9] D. Feng, K. P. Wong, C. M. Wu, and W. C. Siu, "A technique for extracting physiological parameters and the required input function simultaneously from PET image measurements: Theory and simulation study," *IEEE Trans. Info. Tech. Biomed.*, vol. 1, pp. 243–254, 1997.

[10] K. P. Wong, D. Feng, S. R. Meikle, and M. J. Fulham, "Validation of noninvasive quantification technique for neurologic FDG-PET studies," *J. Cereb. Blood Flow Metab.*, vol. 19, no. suppl. 1, pp. S819, 1999.

[11] K. P. Wong, D. Feng, S. R. Meikle, and M. J. Fulham, "Segmentation of dynamic PET images using cluster analysis," in *Conf. Record, IEEE Medical Imaging Conf. 2000*, Lyon, France, October 15–20, 2000, IEEE Publication.

[12] J. Ashburner, J. Haslam, C. Taylor, V. J. Cunningham, and T. Jones, "A cluster analysis approach for the characterization of dynamic PET data," in *Quantification of Brain Function using PET*, R. Myers, V. Cunningham, D. Bailey, and T. Jones, Eds., pp. 301–306. Academic Press, San Diego, 1996.

[13] E. J. Hoffman, P. D. Cutler, W. M. Digby, and J. C. Mazziotta, "3-D phantom to simulate cerebral blood flow and metabolic images for PET," *IEEE Trans. Nucl. Sci.*, vol. 37, pp. 616–620, 1990.

[14] R. A. Hawkins, M. E. Phelps, and S. C. Huang, "Effects of temporal sampling, glucose metabolic rates, and disruptions of the blood-brain barrier on the FDG model with and without a vascular compartment: Studies in human brain tumors with PET," *J. Cereb. Blood Flow Metab.*, vol. 6, pp. 170–183, 1986.